Fluorescent Sodium Alginate Applied to Papermaking Furnish with Polyamideamine Epichlorohydrin

Xiao Ning,[a] Chunli Yao,[a,*] Lina Guan,[b] and Yuanyuan Bai [c]

To explore the distribution of paper strengthening agent polyamideamine epichlorohydrin (PAE)/sodium alginate (SA) binary system in handsheets, SA was labeled by fluorescein isothiocyanate (FITC) to trace the system in paper. 1,6-diaminohexane was used to link SA and FITC to prepare fluorescein isothiocyanate sodium alginate (F-SA), and the optimal synthesis conditions of SA and 1,6-diaminohexane were evaluated. F-SA was identified by ultraviolet (UV) spectral scanning, Fourier transform infrared spectroscopy (FTIR), and fluorescence microscope. The PAE/F-SA binary system in the paper sheet was detected with a fluorescence microscope. The results indicated that FITC could successfully label SA marked as F-SA. The fluorescence substitution degree was 0.89%. Compared with the PAE/SA binary system, the PAE/F-SA binary system produced significant fluorescence in the paper, which indicated that the PAE/SA binary system was evenly distributed and formed a network structure in the handsheets. Furthermore, this method of fluorescence labeling could be employed in papermaking.

Keywords: Sodium alginate; Fluorescent labeling; Fluorescein isothiocyanate; Polyamideamine epichlorohydrin; Paper strengthening agent

*Contact information: a: Beijing Key Laboratory of Lignocellulosic Chemistry, Beijing Forestry University, Beijing 100083 China; b: Affiliated Primary School of Beijing Forestry University, Beijing 100083, China; c:National Engineering Lab for Pulp and Paper, China National Pulp and Paper Research Institute, Beijing 100102, China; *Corresponding author: chunliyao2006@163.com*

INTRODUCTION

In a wide variety of applications, fluorescent tags can be used to produce sensitive, quantitative detection. FITC is a common fluorescent labeling reagent that produces a high fluorescent yield, has a good low temperature coefficient, and is photostable (de Haas *et al.* 2000; He *et al.* 2013). This product of a natural polymer is prepared as a natural fluorescent polymer material, which can also be used for pH sensing and button-loading drugs.

Compared with synthetic polymers, natural polymers are cheaper, more readily available, renewable, biocompatible, and biodegradable. Natural polymers contain a large number of amino or hydroxyl groups that can be easily modified chemically, which broadens the scope of their application (Zhang and Zhang 2010).

Fluorescent materials based on natural polymers have been widely employed in the fields of fluorescence tracing, cell imaging, photoelectric materials, sensing, medicine delivery, *etc*. (Agrawal *et al.* 2010). These applications overcome the limitations of small molecule fluorescent compounds and offer the advantages of easy processing, good mechanical performance, easy synthesis, good corrosion resistance, and low cost. Currently, polysaccharides are widely used in the fields of medicine, food, cosmetics, and

chemistry. As the research and development of polysaccharides continues to advance, application of these materials in the field of fluorescent labeling will also progress (Kobayashi *et al.* 1990; Meunier and Wilkinson 2002). With the development of fluorescent polymer technology and sustainability requirements, the number of applications of natural high molecular fluorescent materials will increase. Natural macromolecular fluorescent materials such as SA ($(C_6H_7O_6N_a)_n$), cellulose, chitosan, protein, and lignin have been extensively studied and applied in the fields of fluorescence tracing, cell imaging, drug carrier, sensors, *etc.* (Abitbol and Gray 2007; Karakawa *et al.* 2007a,b; Chang *et al.* 2009; Iliescu *et al.* 2014; Wang *et al.* 2014).

SA is a widely used natural polysaccharide, but the complexity of the structure and composition of polysaccharides has significantly limited research on this material (Rees and Welsh 1977; Jang *et al.* 1995). Prior research has focused on film forming with other substances, complexes, cross-linking, *etc.* (Zheng *et al.*1998; Braccini *et al.*1999).

SA is a linear natural biological macromolecule that is extracted from algae. It contains a hydroxyl group and a carboxyl group on the same single sugar ring. SA can be used as a food stabilizer, thickener, or emulsifier, and is widely used in industrial products, agriculture, medicine, and food processing. SA can also potentially be used as a fluorescent material (Fei and Gu 2009). For instance, Liu *et al.* (2008) prepared SA functionalized rare earth ions Tb^{3+}/Eu^{3+} hybrid, Eu^{3+}, and Tb^{3+}, that exhibited photoluminescence. SA aerogels and alcohol gels containing Eu^{3+} were found to exhibit the highest quantum yield. A hybrid alginate aerogel, containing Tb^{3+}/Eu^{3+}, was found to exhibit multi-wavelength emission peaks. The choice of the excitation wavelength was found to adjust the fluorescence of the material from red to yellow green. Chaudhary *et al.* (2009) coated fluorescent dyes on natural SA to produce a combination that was used to detect select substances.

In the paper industry, PAE is an ideal wet strength additive. The addition of PAE increases the joint strength between the fibers (Lindström *et al.* 2005). Improvement in the wet strength of paper sheets can be made through the establishment of chemical bonds by fiber-fiber contacts in papermaking. The 3-hydroxy-azetidinium group of PAE can react with the carboxyl groups of cellulose through hetero-crosslinking (Espy 1995). The PAE resin could react with itself and create a network around the fibers (Obokata and Isogai 2009). However, PAE is a cationic polymer. When paper suspension contains excess PAE, wet strength can deteriorate. It seems that the balance of anionic and cationic ions related to zeta potential is a vital factor in the performance of the system (Khosravani and Rahmaninia 2013). To produce products with suitable properties, researchers have developed a wet strength agent sharing technology (Obokata and Isogai 2009; Jang *et al.* 2013; Siqueira *et al.* 2015). This technology centers on producing paper with an improved wet strength by adding one or more wet strength agents (or a wet strength agent and its associated additives) (Ahola *et al.* 2008; Taipale *et al.* 2010; Su *et al.* 2012; Genest *et al.* 2013; Yang *et al.* 2017). To produce sheets with higher wet strength, anionic additives, *e.g.* carboxymethyl cellulose (CMC) or anionic polyacrylamide, are coupled with PAE (Xu *et al.* 1999; Siqueira *et al*. 2013).

SA contains anionic carboxyl groups and is similar to CMC (Guiseley 1989). The main advantages of CMC or SA when compared to cellulose fibers are its high content of carboxyl groups and its water-soluble character. The combined addition of SA and PAE is then a way to adsorb more PAE onto the fibers before reaching the neutralization or saturation of the fiber surface. Alginate found in seawater is a major component of brown seaweed and always exists in its cell wall and matrix as a mixture of the cationic salt

forms (Hernández-Carmona *et al.* 1999). Additionally, the alginate polymers were applied in surface sizing to reduce liquid penetration and increase surface strength (Richardson *et al.* 2003).

Excessive cationic polyelectrolyte in solution forms complexes with subsequently added anionic polymer (Hubbe *et al.* 2003; Hubbe 2007). Through a synergistic effect, the PAE/SA could improve the mechanical properties of the paper sheets compared with the addition of PAE alone. Development of the binary systems to optimize the amount of PAE used in the paper industry shows promise in decreasing the environmental impacts of PAE and further increasing paper strength. The basis for this approach is the alternation of deposition layers. The PAE/SA system shows better wet strength for the sheets, and SEM analysis has shown that the binary system could increase the contact of fibers in paper sheets (Wågberg and Hägglund 2001; Bai *et al.* 2017). The reasons for the improvement of mechanical properties by the addition of a PAE/SA system were analyzed by scanning electron microscopy (SEM), Fourier transform infrared spectroscopy (FTIR), and atomic force microscopy (AFM) (Ferrer *et al.* 2012; He *et al.* 2015; Siqueira *et al.* 2015). These methods just detected the groups (such as ester bonds, CH_2OH stretching mode, amide II and I vibrations, and CH-O-CH_2 stretching) in the sheets and segmental connection between fibers and PAE/SA but could not explain the system effect on dispersion and distribution around the sheets. It is hypothesized that the biopolymer SA coupled with PAE could create a network around the fibers.

In this study, SA was labeled by FITC. Fluorescein isothiocyanate sodium alginate (F-SA) was coupled with PAE as a binary system to cellulose fiber networks that traced how the system combined with fibers to form networks, which became uniformly distributed in the paper. Optimum conditions for the synthesis of F-SA were established. The structure of F-SA was characterized by several methods to better understand the synthetic products.

EXPERIMENTAL

Materials

The commercial SA powder was obtained from Qingdao Xiangyu Seaweed Co. Ltd. (Qingdao, China). The viscosity of SA was 281.5 mPa•s, as determined according to the China GB standard methods (GB/T 14704 (2006)). The FITC and Sephdex G-25 were provided by Beijing LEYBOLD Cable Technology Co. Ltd. (Beijing, China). 1,6-diaminohexane ($NH_2(CH_2)_6NH_2$) and $NaBH_3CN$ were taken from Shanghai HaoYe Chemical Co., LTD. (Shanghai, China). Acetic acid (HAc), sulfuric acid (98 wt%), and phenol were purchased from Beijing Chemical Industry Group Co. (Beijing, China). The cationic PAE used in this study was a commercial product from Xinquan Paper Additives Co. (Taishan, China) in the form of 12.5% water solutions. The mixed waste pulp was obtained from Shandong HUATAI Group. All of the above chemicals were analytical grade and used without further purification.

Preparation of Fluorescein Isothiocyanate Sodium Alginate (F-SA)

Four-hundred milligrams of SA were dissolved in 20 mL 0.5 mol/L $NH_2(CH_2)_6NH_2$ solution with 10% HAc (w/v); 300 mg of $NaBH_3CN$ dissolved in 2 mL of distilled water were slowly added to the SA solution. Then, the mixed solution was placed in a constant temperature water bath at 37 °C and magnetically stirred for 24 h.

After the reaction, the solution was separated by centrifugation at 9,000 RPM for 10 min. The supernatant was dialyzed after being centrifuged at 9,000 r/min for 10 min and purified further through the Sephadex G25 column (made by our laboratory). The outflow fraction (D-SA) was detected with the phenol-sulfuric acid method (Masuko *et al.* 2005) and freeze-dried in a freeze dryer (Shanghai Yu Ming Instrument Co., Ltd, Shanghai, China).

A total of 200 mg of D-SA was weighed and dissolved in 10 mL of distilled water, then adjusted to a pH of 8.5 by 0.5 mol/L $NaHCO_3$. FITC was then added to the solution at room temperature and left to react overnight. Then, the reactant was added to ethanol at 80% final concentration. There was a large amount of bright yellowish-green precipitate, and centrifugation was needed to collect the precipitate. The precipitate was dissolved into water and precipitated with ethanol three times. After being concentrated and purified through the Sephadex G25 column, the corresponding components marked as F-SA were collected after being freeze-dried and stored at -50 °C for further use (Su *et al* .2013; Li *et al.* 2014).

Factors of Fluorescence Labeling

The linking of $NH_2(CH_2)_6NH_2$ to SA was the critical step to ensure that the fluorescent label could be linked to the SA. The main factors that controlled this reaction were the reaction time, temperature, dosage of $NaBH_3CN$, the volume of $NH_2(CH_2)_6NH_2$ with HAc, and the pH of the solution. In order to obtain the optimum conditions for the production of D-SA and to verify the effect of each factor on the reaction, the reaction conditions were controlled. These conditions included reaction time (6 h, 12 h, 24 h, 36 h, and 48 h), temperature (20 °C, 35 °C, 50 °C, 65 °C, and 80 °C), the amount of $NaBH_3CN$ that is ratio between $NaBH_3CN$ to SA (1: 4, 3: 4, 5: 4, 7: 4, and 9: 4), the volume ratio of $NH_2(CH_2)_6NH_2$ with 10% HAc (1: 0.25, 1: 0.5, 1: 1, 1: 1.5, 1: 2 (v/v)), and the pH of the solution by HAc , ranging from 7.5 to 9.5 (7.5, 8.0, 8.5, 9.0, and 9.5).

Preparation of the Paper Sheets

The pulp fibers (1.57 wt%) were beaten from to 40 °SR. An aqueous pulp suspension was obtained in a pulp disintegrator. The concentration of the pulp slurry was 16 g/L. Standard handsheets (80 g/m^2) were prepared in accordance with the China GB standard methods (GB/T 451.2 (2002)). With a dry pulp mass of 2.512 g, 0.8% PAE was added into the pulp suspension to stir at 500 rpm for 5 min, then 0.5% SA or F-SA solution was added to stir for 10 min. The handsheets were pressed at 430 kPa for 4 min and then air dried under restrain at 105 °C for 3 min. The dried paper sheets were conditioned at 23 °C and 50% RH for at least 24 h before being tested.

Measurements and Analyses of Paper Sheets

The wet tensile index of the hand sheet strength was tested following the TAPPI T 220 method. It is defined as the quotient of the tensile strength (N/m) and the basis weight (g/m^2) of the paper and thus its unit is N·m/g.

Characterization

The concentration of polysaccharide

The concentration of polysaccharide in the solutions was determined using the phenol-sulfuric acid method (Russell *et al.* 1998). A regression equation was used to determine the concentration of polysaccharide of F-SA. The stock solution of glucose

solution (0.04 mg/mL) was then prepared. A standard solutions series with concentrations ranging from 0.32 to 0.64 μg/mL was prepared by diluting the stock solution. 1.0 mL of 6 wt% phenol and 5.0 mL of 98 wt% sulfuric acid were added in 2.0 mL standard solution, then the solution was shaken and cooled for 20 min. The absorbance was measured at 490 nm by UV-2401PC (Bruker, Karlsruhe, Germany) and a standard curve was made. Then 2.0 mL for 1 wt% SA solution was evaluated; the absorbance was read three times, as was done for glucose solutions. The polysaccharide content was calculated using the regression equation.

Determination of fluorescent substitution

To determine the marked efficiency of SA with FITC, a regression equation was made. The FITC solutions were prepared at concentrations of 0.01, 0.02, 0.03, 0.04, and 0.05 μg/mL. The process was carried out in the absence of light. The fluorescence intensity of each tube was measured using a fluorescence spectrophotometer (E_x = 495 nm; E_m= 495 nm) (Spectra Max M5, Molecular Devices, California, USA), with distilled water set as a blank control. The standard curve was drawn, with FITC concentration as the horizontal coordinate, while fluorescence intensity absorbance was the ordinate.

The sample solution was made using the F-SA (5 μg/mL) solutions. The fluorescence intensity of F-SA was measured, and the substitution degree was calculated using the regression equation (Su *et al.* 2013).

Ultraviolet (UV) spectral scanning

SA, D-SA and F-SA were separately dissolved in a phosphate buffer at 1 mg/mL. All solutions were scanned from 200 nm to 800 nm by UV-2401PC (Bruker).

Fourier transform infrared spectroscopy

Fourier transform infrared (FT-IR) spectrums of the SA, D-SA and F-SA samples were obtained using a Thermo Scientific NicoletN10 FT-IR spectrometer (Madison, WI, USA). Two-hundred milligrams SA, D-SA, and F-SA were separately mixed with 200 mg of dried KBr powder, ground, and then pressed into 1 mm pellets for FT-IR measurement in a frequency range of 4000 cm^{-1} to 400 cm^{-1}.

Fluorescence microscopy

The fluorescence microscope images of the paper sheets were obtained on a DM2500 (Leica, Wetzlar, Germany) fluorescence microscope.

RESULTS AND DISCUSSION

Preparation of F-SA

The synthesis process and chemical structures are illustrated in Fig. 1. SA did not react with FITC directly through reductive amination, because it does not contain an amino group. Therefore, $NH_2(CH_2)_6NH_2$ was used as a suitable linker (Li *et al.* 2014). The aldehyde of the reducing end of the SA reacted with $NH_2(CH_2)_6NH_2$, producing the SA derivative D- SA. The purified D-SA reacted with FITC at weak alkaline conditions, yielding F- SA.

The Concentration of Polysaccharide

A regression equation was obtained for glucose content based on the absorbance value of the solution using a UV-Vis spectrophotometer. The regression equation used to calculate the glucose concentration was y = 0.9988x-0.203 (R^2 = 0.9950) (Fig. 2) with glucose content as the horizontal coordinate, while fluorescence intensity was the ordinate. The resulting increase in FITC fluorescence is proportional to the concentration of glucose (Russell *et al.* 1998; Cuesta *et al.* 2003). Therefore, the concentration of polysaccharide was found to be 65.47%.

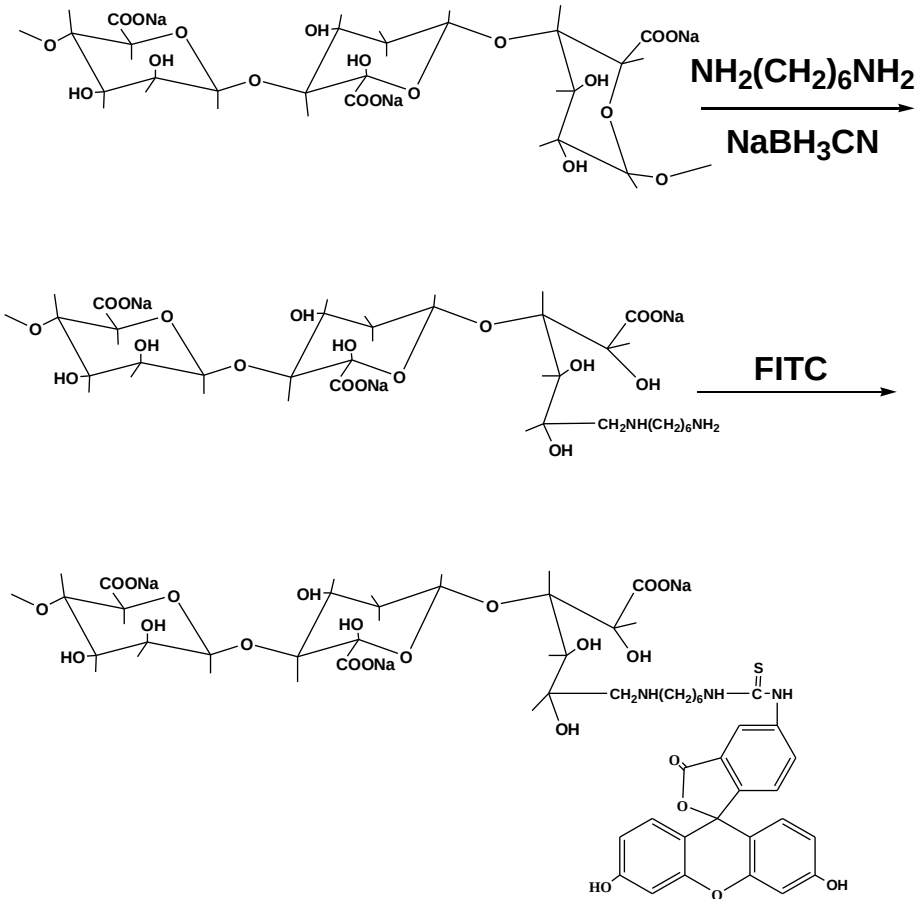

Fig. 1. The fluorescence labeling process of F-SA and its chemical structure

Factors of F-SA Labeling

In the study of the fluorescent labeling of SA, the attachment of $NH_2(CH_2)_6NH_2$ to SA was the critical step in ensuring that the fluorescent label could be attached to the SA. Several experiment factors (Rees and Welsh 1977; Chang *et al.* 2009) were studied, including the reaction time, $NaBH_3CN$ dosage (Iliescu *et al.* 2014), temperature, HAc, and pH. Set reaction conditions were the following: temperature (35 °C), reaction time (24 h), the ratio between $NaBH_3CN$ and SA (3: 4 w/w), the ratio between 1,6 hexanediamine and HAc (1: 0.5 v/v), and pH=8.0. This study used the control variable method and the following sections discuss these factors in detail. Figure 3 shows the products obtained by different factors, which were the horizontal coordinate and the absorbance was the ordinate.

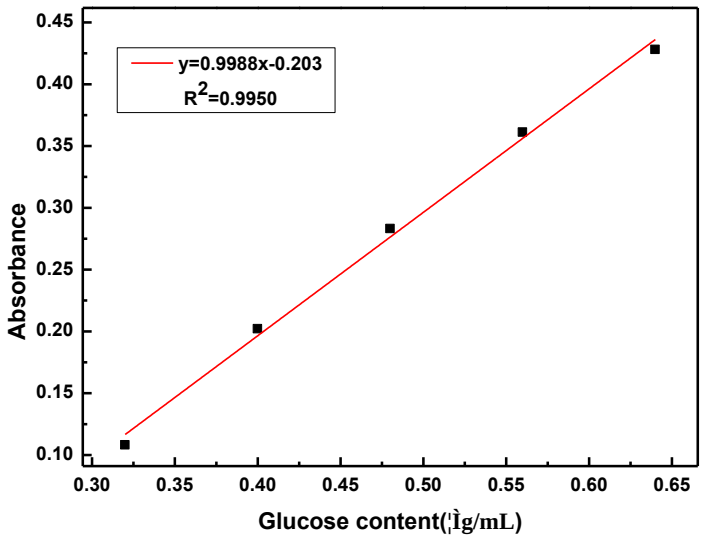

Fig. 2. The standard curve of glucose

Effect of reaction time

As the reaction time increased, the absorbance of the resulting dissolved product at 320 nm increased (Fig. 3(a)). This indicated that longer reaction time resulted in more products. The reason for that may be that the increased frequency of contact between SA and the $NH_2(CH_2)_6NH_2$ was beneficial to obtain the desired product. Moreover, the solution's viscosity became noticeably higher as the reaction time increased. Sufficient reaction time is needed for the $NH_2(CH_2)_6NH_2$ to fully react with the SA, thereby facilitating the completion of the synthesis reaction.

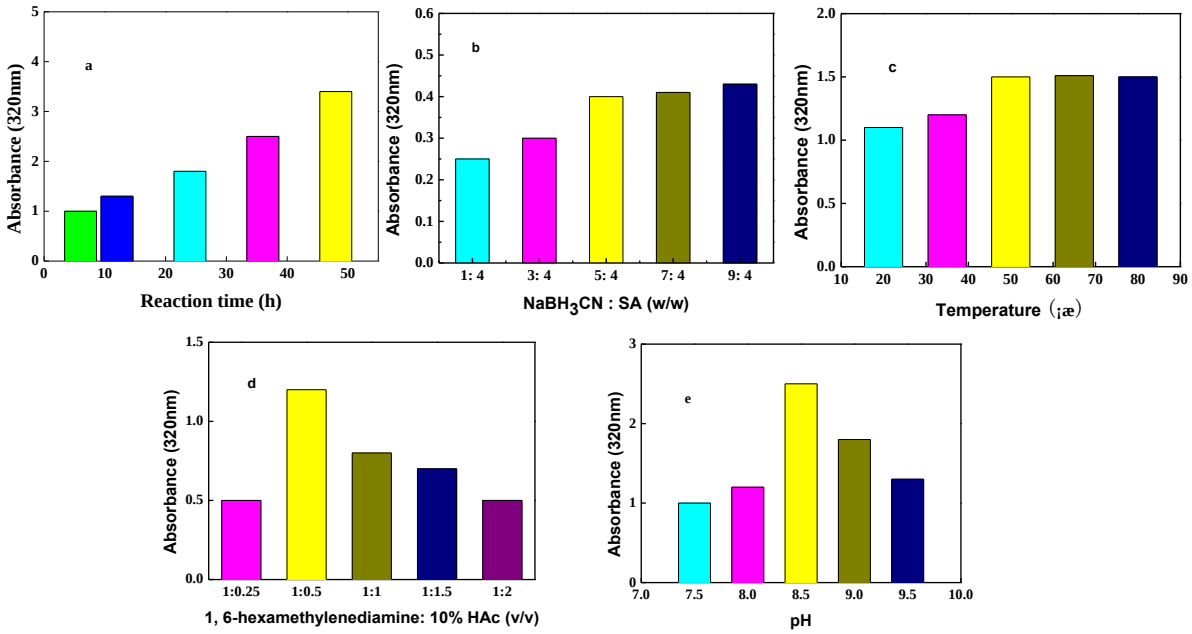

Fig. 3. Factors of SA fluorescent labeling: (a) reaction time; (b) $NaBH_3CN$; (c) temperature; (d) HAc; (e) pH

Effect of $NaBH_3CN$

$NaBH_3CN$ was used as a mild reducing agent to catalyze synthesis (Iliescu *et al.* 2014). As shown in Fig. 3(b), the absorbance of the reaction solution increased as the quantity of $NaBH_3CN$ was increased. This showed that the content of $NaBH_3CN$ in solution had a positive effect on reaction efficiency. However, the dosage of $NaBH_3CN$ had little effect on the reaction compared with others. Therefore, it appeared that the $NaBH_3CN$ was a reaction catalyst, but, if present in higher concentrations, the absorbance did not increase much. Therefore, the ratio of $NaBH_3CN$ and SA was maintained at 1:4 (w/w) to achieve comparative economy (the consumption of SA in this experiment was 400 mg).

Effect of temperature

Figure 3(c) shows the effect of the reaction temperature on yield. Both spectral responses and protolytic constants were found to depend on temperature (Sjöback *et al.* 1995). As the temperature was raised, the absorbance was higher. Temperature raised was facilitated the contact between the reactants. It can reach the highest absorbance at 50 °C. However, the absorbance at 65 °C was no longer increased and decreased slightly at 80 °C. Therefore, it can reach the highest absorbance at 50 °C under the most economical conditions. Increasing the temperature increases the energy consumption. So it was judged that the optimum solution temperature was 50 °C.

Effect of HAc dosage

In the reaction between SA and $NH_2(CH_2)_6NH_2$, HAc was used to accelerate the dissolution of SA and adjust the pH. Figure 3(d) shows that when the ratio was 1:0.5, the value reached a peak that was conducive to the reaction. But by continued addition of HAc, the absorbance decreased. The likely reason is that the complete dissolution of the SA requires sufficient HAc, and when the ratio was 1:0.5 (v/v), the pH of the solution was 8.5, the dosage of HAc was sufficient to dissolve the SA. However, the amount of HAc continued to increase, the pH decreased, the amino group in the 1, 6-hexanediamine exists in the form of $-NH_3^+$, which is unfavorable for the reaction. Therefore, the ratio should be controlled at 1:0.5 (v/v), to produce the best reaction conditions.

Effect of pH

The two NH_2 groups in $NH_2(CH_2)_6NH_2$ are able to react with the reductive terminal aldehyde group in the SA in an alkaline environment. The UV-vis absorption spectrum of FITC is strongly affected by pH (Sjöback *et al.* 1995). Therefore, the concentration of amino groups ($-NH_2$) in solution determined the reaction efficiency. As the pH was increased, the concentration of 2-NH_2 in the solution and the reaction rate increased, which favored the fluorescence reaction.

Figure 3(e) shows that when the pH was 8.5, the reaction had the best result. When the pH was lower than 7, the amino acids in the solution were mainly in the form of $-NH^{3+}$, which was not conducive to the desired reaction. With the increase of solution pH, the concentration of $-NH_2$ in solution increased, and the absorbance increased. When the pH value was 8.5, the reaction had best performance. When the pH value was more than 8.5, the absorbance decreased, meaning that the optimal pH is 8.5.

Characterization of F-SA

Determination of degree of fluorescence substitution

The fluorescence substitution degree of the solution was related to the solvent, solution temperature, and pH, and also related to the absorption intensity of the solution and the fluorescence efficiency of the fluorescent product. As shown in Fig. 4, the regression equation y = 12106x - 2.14 (R^2 = 0.9905) was calculated to reflect the relationship between the two parameters. The standard curve was drawn, with FITC concentration as the horizontal coordinate, while fluorescence intensity was the ordinate. The fluorescence intensity was calculated to be 0.89% using this equation (Su *et al.* 2013).

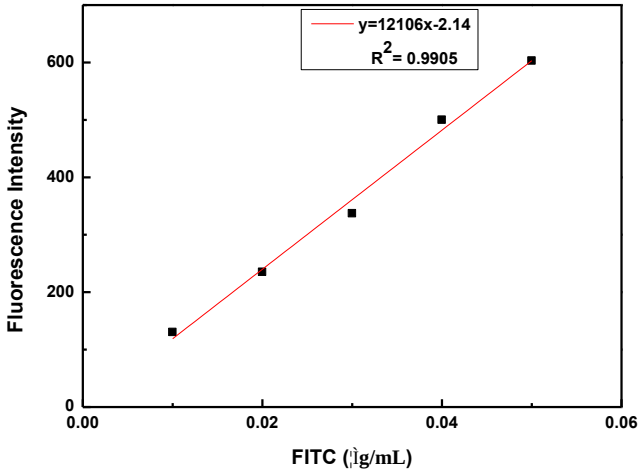

Fig. 4. The standard curve of FITC

As shown in Fig. 5, the fluorescence intensity of the samples varied.

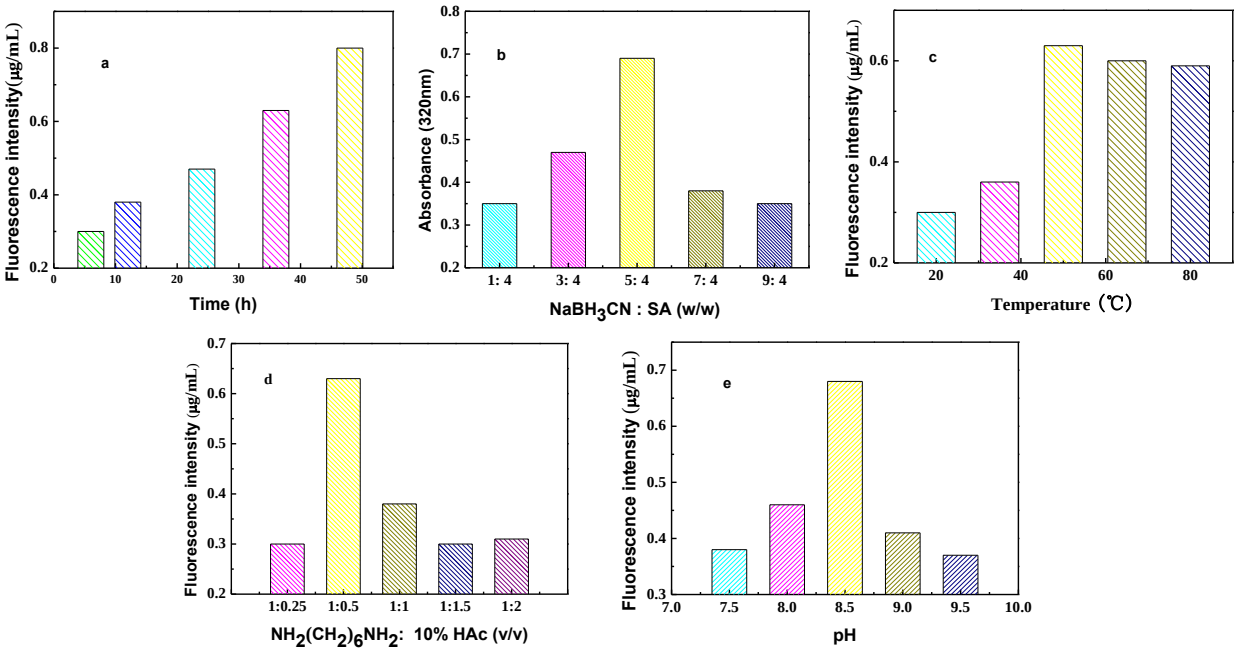

Fig. 5. The label fluorescence efficiency of synthetic products (a) time; (b)$NaBH_3CN$; (c) temperature, (d) 10% HAc; (e) pH

More effective fluorescence labeling of the SA resulted in higher fluorescence readings. According to the standard curve, the products obtained by different factors were as the horizontal coordinate, while fluorescence intensity was the ordinate. The highest fluorescence intensity of the samples, as well as the absorbance of the D-SA, was found at 320 nm. The best reaction conditions reflected by the fluorescence intensity were the same as those obtained in the single factor investigation of the D-SA synthesis reaction. This indicated that the relative reaction between SA and $NH_2(CH_2)_6NH_2$ significantly affected the efficiency of the labeling of the SA. The bonding of $NH_2(CH_2)_6NH_2$ to the SA was critical to the success of this experiment.

Ultraviolet (UV) spectral scanning

Figure 6 compares the UV-Vis spectra of SA, D-SA, and F-SA. SA did not show any absorption peaks at 320 nm and 490 nm, and the UV absorption peak of D-SA occurred at 320 nm. There was a significant difference between D-SA and the physical mixture of SA. The spectrum of F-SA showed absorption maxima of the dianionic (490 nm) form of FITC (Sjöback 1995; Dong and Roman 2007). It can be inferred that FITC had been successfully connected to SA.

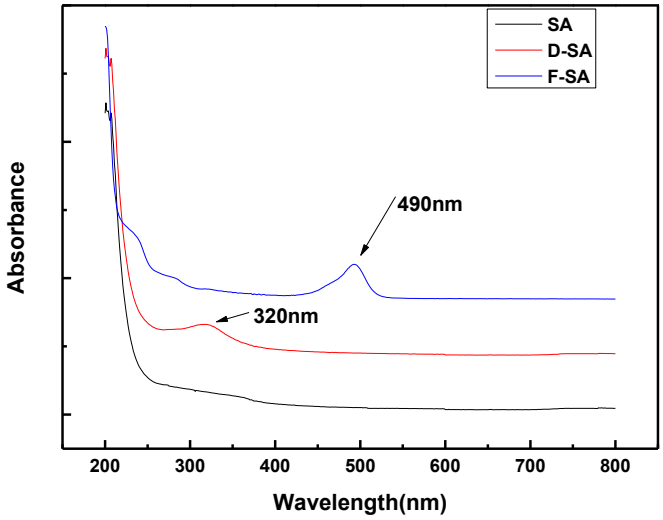

Fig. 6. UV-Vis spectra of SA (black), D-SA (red) and F-SA (blue)

Fourier transform infrared spectroscopy

Because the fluorescence labeling efficiency of F-SA was only 0.89%, the labeling reagent linked to the reducing end of SA did not affect its backbone structure. Therefore, the related $NH_2(CH_2)_6NH_2$ and FITC signals were weak in the FT-IR spectrum. As shown in Fig. 7, the peak of the $\nu_{N\text{-}H}$ of D-SA and F-SA was covered by a broad strong peak of $\nu_{O\text{-}H}$ of SA at around 3431 cm^{-1}. There was a variation at about 3431 cm^{-1} that did not appear in the spectrum of D-SA and F-SA. Because the ring was broken, the $\nu_{O\text{-}H}$ of D-SA and F-SA may produce hydrogen bonding and forming multiplet peaks between 3000 and 2500 cm^{-1}. And the strong carboxylate ion band (1637 cm^{-1}) also covered the weak absorbance of $\delta\nu_{N\text{-}H}$ in $NH_2(CH_2)_6NH_2$ and in the skeletal vibrations of aromatic ring in FITC. These findings indicated that the main skeletons of SA, D-SA, and F-SA were almost the same (Li *et al.* 2014).

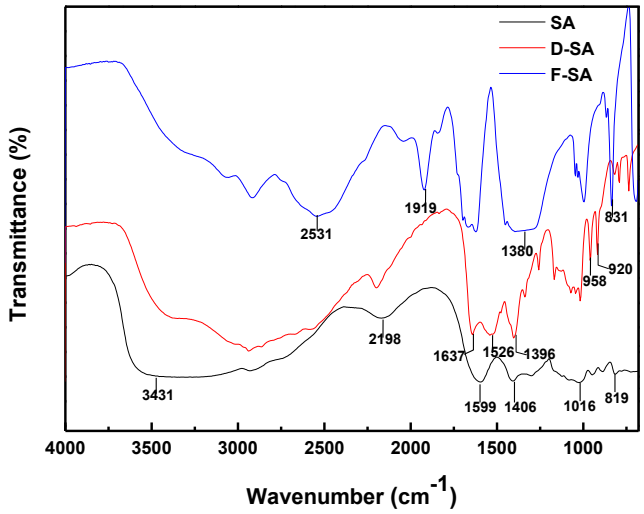

Fig. 7. FT-IR spectra of SA (black), D-SA (red) and F-SA (blue)

Fluorescence Microscope Scan

The distribution of the PAE/F-SA binary wet strength system in handsheets was studied using a fluorescence microscope (Fig. 8). SA was coupled with PAE relating to zeta potential, SA was coupled with PAE relating to zeta potential. A PAE/SA binary system can significantly improve the mechanical properties of paper sheets (Bai *et al.* 2017). And the wet tensile strength of paper with PAE/F-SA binary system was 22.3 N·m/g, while the PAE alone and control were 14.0 N·m/g and 1.5 N·m/g, respectively. It seems that the balance of anionic and cationic ions related to zeta potential is a vital factor in the performance of system (Khosravani and Rahmaninia 2013; Rahmaninia *et al.* 2018). Methods such as FTIR, AFM, and SEM are used to analyze paper composition (Ferrer *et al.* 2012; He *et al.* 2015; Siqueira *et al.* 2015), but these methods cannot analyze the distribution of additives in paper. As shown in Fig. 8, F-SA provided significant fluorescence in paper because of the use of FITC and implied homogeneous distribution. Because the PAE linked to F-SA, it can be inferred that the PAE/SA binary system was distributed homogeneously in the sheets. It is possible that SA coupled with PAE could create a network structure around the fibers. Overall, it is possible to improve the mechanical properties of the paper sheets.

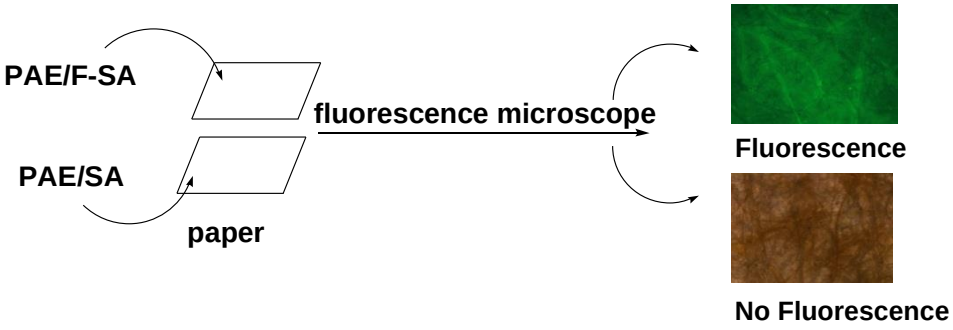

Fig. 8. Paper sheets imaging by fluorescence microscope

CONCLUSIONS

1. The SA was successfully labeled by fluorescein isothiocyanate (FITC) to produce fluorescein isothiocyanate sodium alginate (F-SA). The synthesis of F-SA exhibited good synthetic efficiency under the following reaction conditions: the pH in solution was 8.5, the temperature 50 °C, the mass of $NaBH_3CN$ was 25% SA, and the reaction time was 48 h. Based on the results of UV-Vis and FTIR, the reaction with SA could produce F-SA. The results indicated that FITC could label SA, and the fluorescence substitution degree was 0.89%.
2. Fluorescence microscopy showed that the binary system with polyamideamine epichlorohydrin (PAE) and F-SA binary system could become evenly distributed in the paper. It is possible that SA coupled with PAE could create a network structure around the fibers. Hence, it is possible that fluorescence labeling system could be employed in papermaking to improve the mechanical properties of the handsheets,

ACKNOWLEDGMENTS

The authors thank the National Science Foundation of China (31470605) for financial support.

REFERENCES CITED

Abitbol, T., and Gray, D. (2007). "CdSe/ZnS QDs embedded in cellulose triacetate films with hydrophilic surfaces," *Chem. Mater.* 19(17), 4270-4276. DOI: 10.1021/cm0704332

Ahola, S., Österberg, M., and Laine, J. (2008). "Cellulose nanofibrils—Adsorption with poly (amideamine) epichlorohydrin studied by QCM-D and application as a paper strength additive," *Cellulose,* 15(2), 303-314. DOI: 10.1007/s10570-007-9167-3

Agrawal, P., Strijkers, G. J., and Nicolay, K. (2010). "Chitosan-based systems for molecular imaging," *Adv. Drug Deliv. Rev.* 62(1), 42-58. DOI: 10.1016/j.addr.2009.09.007

Braccini, I., Grasso, R. P., and Pérez, S. (1999). "Conformational and configurational features of acidic polysaccharides and their interactions with calcium ions: a molecular modeling investigation," *Carbohyd. Res.* 317(1-4), 119-130. DOI: 10.1016/S0008-6215(99)00062-2

Bai, Y. Y., Lei, Y. H., Shen, X. J., Luo, J., Yao, C. L., and Sun, R. C. (2017). "A facile sodium alginate-based approach to improve the mechanical properties of recycled fibers," *Carbohyd. Polym.* 174, 610-616. DOI: 10.1016/j.carbpol.2017.06.091

Cohen, S., Lobel, E., Trevgoda, A., and Peled, Y. (1997). "A novel *in situ*-forming ophthalmic drug delivery system from alginates undergoing gelation in the eye," *J. Controlled Release* 44(2-3), 201-208. DOI: 10.1016/S0168-3659(96)01523-4

Cuesta, G., Suarez, N., Bessio, M. I., Ferreira, F., and Massaldi, H. (2003). "Quantitative determination of pneumococcal capsular polysaccharide serotype 14 using a modification of phenol–sulfuric acid method," *J. Microbiol. Methods* 52(1), 69-73. DOI: 10.1016/S0167-7012(02)00151-3

Chang, C., Peng, J., Zhang, L., and Pang, D.-W. (2009). "Strongly fluorescent hydrogels with quantum dots embedded in cellulose matrices," *J. Mater. Chem.* 19(41), 7771-7776. DOI: 10.1039/b908835k

Chaudhary, A., Raina, M., Harma, H., Hanninen, P., McShane, M. J., and Srivastava, R. (2009). "Evaluation of glucose sensitive affinity binding assay entrapped in fluorescent dissolved-core alginate microspheres," *Biotechnol. Bioeng.* 104(6), 1075-1085. DOI: 10.1002/bit.22500

de Haas, C. J., van Leeuwen, H. J., Verhoef, J., van Kessel, K. P., and van Strijp, J. A. (2000). "Analysis of lipopolysaccharide (LPS)-binding characteristics of serum components using gel filtration of FITC-labeled LPS," *J. Immunol. Methods* 242(1-2), 79-89. DOI: 10.1016/S0022-1759(00)00207-6

Dong, S., and Roman, M. (2007). "Fluorescently labeled cellulose nanocrystals for bioimaging applications," *J. Am. Chem. Soc.* 129(45), 13810-13811. DOI: 10.1021/ja076196l

Espy, H. H. (1995). "The mechanism of wet-strength development in paper: A review," *Tappi J.* 78, 90-99.

Fei, X., and Gu, Y. (2009). "Progress in modifications and applications of fluorescent dye probe," *Prog. Nat. Sci.* 19(1), 1-7. DOI: 10.1016/j.pnsc.2008.06.004

Ferrer, A., Filpponen, I., Rodríguez, A., Laine, J., and Rojas, O. J. (2012). "Valorization of residual Empty Palm Fruit Bunch Fibers (EPFBF) by microfluidization: Production of nanofibrillated cellulose and EPFBF nanopaper," *Bioresource Technol.* 125, 249-255. DOI: 10.1016/j.biortech.2012.08.108

Guiseley, K. B. (1989). "Chemical and physical properties of algal polysaccharides used for cell immobilization," *Enzyme Microb. Technol.* 11(11), 706-716. DOI: 10.1016/0141-0229(89)90119-1

Genest, S., Salzer, R., and Steiner, G. (2013). "Molecular imaging of paper cross sections by FT-IR spectroscopy and principal component analysis," *Anal. Bioanal. Chem.* 405(16), 5421-5430. DOI: 10.1007/s00216-013-6967-1

Hernández-Carmona, G., McHugh, D. J., and López-Gutiérrez, F. (1999). "Pilot plant scale extraction of alginates from *Macrocystis pyrifera*. 2. Studies on extraction conditions and methods of separating the alkaline-insoluble residue," *J. Appl. Phycology* 11(6), 493-502. DOI: 10.1023/A:1008114709681

Hubbe, M. A., Jackson, T. L., and Zhang, M. I. N. (2003). "Fiber surface saturation as a strategy to optimize dual-polymer dry strength treatment," *Tappi J.* 2(11), 7-12.

Hubbe, M. A. (2007). "Bonding between cellulosic fibers in the absence and presence of dry-strength agents – A review," *BioResources* 1(2), 281-318. DOI: 10.15376/biores.1.2.281-318

He, X., Hu, C., Guo, Q., Wang, K., Li, Y., and Shangguan, J. (2013). "Rapid and ultrasensitive *Salmonella Typhimurium* quantification using positive dielectrophoresis driven on-line enrichment and fluorescent nanoparticleslabel," *Biosensors and Bioelectronics* 42, 460-466. DOI: 10.1016/j.bios.2012.11.020

He, W., Yang, T., Wang, Y., and Song, X. (2015). "Carboxymethylation of corncob holocellulose and its influences on paper properties," *J. Wood Chem. Technol.* 35(2), 137-145. DOI: 10.1080/02773813.2014.902963

Iliescu, R. I., Andronescu, E., Ghitulica, C. D., Voicu, G., Ficai, A., and Hoteteu, M. (2014). "Montmorillonite–alginate nanocomposite as a drug delivery system–incorporation and in vitro release of irinotecan," *Int. J. Pharm.* 463(2), 184-192. DOI: 10.1016/j.ijpharm.2013.08.043

Jang, L. K., Nguyen, D., and Geesey, G. G. (1995). "Selectivity of alginate gel for Cu vs Co," *Water Res.* 29(1), 307-313. DOI: 10.1016/0043-1354(94)E0090-S

Jang, Y., Lee, H., and Kang, H. J. (2013). "Physical properties of poly (vinyl alcohol) with polyamide-epichlorohydrin as a wet strength additive for paper," *Polym. Korea* 37(6), 730-735. DOI: 10.7317/pk.2013.37.6.730

Karakawa, M., Chikamatsu, M., Nakamoto, C., Maeda, Y., Kubota, S., and Yase, K. (2007a). "Organic light-emitting diode application of fluorescent cellulose as a natural polymer," *Macromol. Chem. Phys.* 208(18), 2000-2006. DOI: 10.1002/macp.200700154

Karakawa, M., Chikamatsu, M., Yoshida, Y., Azumi, R., Yase, K., and Nakamoto, C. (2007b). "Organic memory device based on carbazole-substituted cellulose," *Macromol. Rapid Commun.* 28(14), 1479-1484. DOI: 10.1002/marc.200700186

Khosravani, A., and Rahmaninia, M. (2013). "The potential of nanosilica–cationic starch wet end system for applying higher filler content in fine paper," *BioResources* 8(2), 2234-2245. DOI: 10.15376/biores.8.2.2234-2245

Kobayashi, M., Urayama, T., and Ichishima, E. (1990). "Fluorescent derivatives of polysaccharide dialdehyde as substrates for glucanases," *Agricultural and Biological Chemistry* 54(7), 1711-1718. DOI: 10.1080/00021369.1990.10870203

Lindström, T., Wågberg, L., and Larsson, T. (2005, September). "On the nature of joint strength in paper – A review of dry and wet strength resins used in paper manufacturing," in*: Proceedings of 13th Fundamental Research Symposium*, Cambridge, UK, pp. 457-562.

Liu, F., Carlos, L. D., Ferreira, R. A., Rocha, J., Gaudino, M. C., Robitzer, M., and Quignard, F. (2008). "Photoluminescent porous alginate hybrid materials containing lanthanide ions," *Biomacromolecules* 9(7), 1945-1950. DOI: 10.1021/bm8002122

Li, P., Li, C., Xue, Y., Zhang, Y., Liu, H., Zhao, X., and Guan, H. (2014). "Preparation, characterization and pharmacokinetics of fluorescence labeled propylene glycol alginate sodium sulfate," *J. Ocean U. China* 13(4), 683-690. DOI: 10.1007/s11802-014-2273-6

Meunier, F., and Wilkinson, K. J. (2002). "Nonperturbing fluorescent labeling of polysaccharides," *Biomacromolecules* 3(4), 857-864. DOI: 10.1021/bm0255241

Masuko, T., Minami, A., Iwasaki, N., Majima, T., Nishimura, S. I., and Lee, Y. C. (2005). "Carbohydrate analysis by a phenol–sulfuric acid method in microplate format," *Anal. Biochem.* 339(1), 69-72. DOI: 10.1016/j.ab.2004.12.001

Obokata, T., and Isogai, A. (2009). "Wet-strength development of cellulose sheets prepared with polyamideamine-epichlorohydrin (PAE) resin by physical interactions," *Nord. Pulp Pap. Res. J.* 24(2), 135-140. DOI: 10.3183/NPPRJ-2009-24-02-p135-140

Rahmaninia, M., Rohi, M., Hubbe, M. A., Zabihzadeh, S. M., and Ramezani, O. (2018). "The performance of chitosan with bentonite microparticles as wet-end additive system for paper reinforcement," *Carbohyd Polym.* 179, 328-332. DOI: 10.1016/j.carbpol.2017.09.036

Rees, D. A., and Welsh, E. J. (1977). "Secondary and tertiary structure of polysaccharides in solutions and gels," *Angewandte Chem. Int. Ed.* 16(4), 214-224. DOI: 10.1002/anie.197702141

Russell, R., Pishko, M., Gefrides, C., and Cote, G. (1998). "A fluorescent glucose assay using poly-L-lysine and calcium alginate microencapsulated TRITC-succinyl-concanavalin A and FITC-dextran," in: *Engineering in Medicine and Biology Society,*

1998. Proc. 20th Annual International Conf. IEEE 6, Texas, USA, pp. 2858-2861.

Richardson, P. H., Trksak, R. M., Tsai, J. J., and Weisser, E. M. (2003). "Degraded hydrophobic, particulate starches and their use in paper sizing," U.S. Patent No. 6,521,088.

Siqueira, E., Naoui, W., Marlin, N., Schott, S., and Mauret, E. (2013). "Effect of chemical additives on the degradation of polyamideamine-epichlorohydrin (PAE) films and PAE-based papers made from bleached kraft pulps," *Nord. Pulp Pap. Res. J.* 28(4), 529-540. DOI: 10.3183/NPPRJ-2013-28-04-p529-540

Siqueira, E. J., Salon, M. C. B., Belgacem, M. N., and Mauret, E. (2015). "Carboxymethylcellulose (CMC) as a model compound of cellulose fibers and polyamideamine epichlorohydrin (PAE)-CMC interactions as a model of PAE – fibers interactions of PAE-based wet strength papers," *J. Appl. Polym. Sci.* 132(26). DOI: 10.1002/app.42144

Sjöback, R., Nygren, J., and Kubista, M. (1995). "Absorption and fluorescence properties of fluorescein," *Spectrochimica Acta Part A: Molecular and Biomolecular Spectroscopy* 51(6), L7-L21. DOI: 10.1016/0584-8539(95)01421-P

Su, Y. L., Hu, J., and Li, Y. T. (2013). "Preparation of fluorescent polysaccharides from *Ganoderma applanatum* and cellular localization on splenic lymphocytes of mice," *J. China Agr. Univ.* 18,147-152.

Su, J., Mosse, W. K., Sharman, S., Batchelor, W., and Garnier, G. (2012). "Paper strength development and recyclability with polyamideamine-epichlorohydrin (PAE)," *BioResources* 7(1), 0913-0924.7: 0913-0924. DOI: 10.15376/biores.7.1.0913-0924

Taipale, T., Holappa, S., Ahlgren, J., Cecchini, J., and Laine, J. (2010). "Interactions of thermo mechanical pulp fractions with high molar mass cationic polyacrylamides: Part 1. Adsorption," *Nord. Pulp Pap. Res. J.* 25(3), 300-309. DOI: 10.3183/NPPRJ-2010-25-03-p300-309

Wågberg, L., and Hägglund, R. (2001). "Kinetics of polyelectrolyte adsorption on cellulosic fibers," *Langmuir* 17(4), 1096-1103. DOI: 10.1023/A:1008114709681

Wang, X. Y., Jin, Z. H., Gan, B. W., Lv, S. W., Xie, M., and Huang, W. H. (2014). "Engineering interconnected 3D vascular networks in hydrogels using molded sodium alginate lattice as the sacrificial template," *Lab Chip* 14(15), 2709-2716. DOI: 10.1039/C4LC00069B

Xu, Y., Yang, C. Q., and Chen, C. M. (1999). "Wet reinforcement of paper with high-molecular-weight multifunctional carboxylic acid," *Tappi J.* 82(8).

Yang, W., Bian, H., Jiao, L., Wu, W., Deng, Y., and Dai, H. (2017). "High wet-strength, thermally stable and transparent TEMPO-oxidized cellulose nanofibril film via cross-linking with poly-amide epichlorohydrin resin," *RSC Adv.* 7(50), 31567-31573. DOI: 10.1039/C7RA05009G

Zhang, J., and Zhang, J. (2010). "Advanced functional materials based on cellulose," *Acta Polymerica Sinica* 12, 1376-1398. DOI: 10.3724/SP.J.1105.2010.10238

Zheng, H., Zhang, H., Zhang, Q., Konno, M., Yang, S., and Wang, J. (1998). "Salt effects on the cross-linking mechanism of cupric-induced sol-gel transition in alginate solutions," *Carbohyd. Polym.* 35(3-4), 215-221. DOI: 10.1016/S0144-8617(97)00248-8

Article submitted: April 20, 2018; Peer review completed: June 28, 2018; Revised version received and accepted: July 27, 2018; Published: August 21, 2018.
DOI: 10.15376/biores.13.4.7519-7533